

# Enhancing Action Recognition by Leveraging the Hierarchical Structure of Actions and Textual Context

Manuel Benavent-Lledo<sup>a,\*</sup>, David Mulero-Perez<sup>a</sup>, David Ortiz-Perez<sup>a</sup>,  
Jose Garcia-Rodriguez<sup>a</sup> and Antonis Argyros<sup>b</sup>

<sup>a</sup>Department of Computer Technology, University of Alicante, Alicante, Spain

<sup>b</sup>Institute of Computer Science, FORTH, Heraklion, Crete, Greece

\*Corresponding author: mbenavent@dtic.ua.es

**Abstract**—We propose a novel approach to improve action recognition by exploiting the hierarchical organization of actions and by incorporating contextualized textual information, including location and previous actions, to reflect the action’s temporal context. To achieve this, we introduce a transformer architecture tailored for action recognition that employs both visual and textual features. Visual features are obtained from RGB and optical flow data, while text embeddings represent contextual information. Furthermore, we define a joint loss function to simultaneously train the model for both coarse- and fine-grained action recognition, effectively exploiting the hierarchical nature of actions. To demonstrate the effectiveness of our method, we extend the Toyota Smarthome Untrimmed (TSU) dataset by incorporating action hierarchies, resulting in the *Hierarchical TSU dataset*, a hierarchical dataset designed for monitoring activities of the elderly in home environments. An ablation study assesses the performance impact of different strategies for integrating contextual and hierarchical data. Experimental results demonstrate that the proposed method consistently outperforms SOTA methods on the Hierarchical TSU dataset, Assembly101 and IkeaASM, achieving over a 17% improvement in top-1 accuracy.

**Index Terms**—Action Recognition, Action Hierarchies, Action Context, Vision-Language Transformer

## I. INTRODUCTION

Recognizing actions in video sequences has become a fundamental task in a wide range of real-world applications, particularly in assistive technologies that enhance safety, efficiency, and quality of life. These technologies are increasingly integral to diverse domains, including video surveillance [1], autonomous driving [2], [3], and human-robot interaction [4]. Specifically, video monitoring systems, such as smarthomes and robots, stand to benefit immensely from these advances. These systems have the potential to significantly improve the quality of life for older adults in domestic environments and enhance worker safety in industrial settings, thereby driving innovation in both healthcare and industrial safety.

In some of these cases, the effectiveness of the provided solutions depends on their ability to operate online and in real-time. In other scenarios, however, offline analysis of behavior may be sufficient. In such cases, considering the broader context provided by the entire video can improve

model performance. For example, routine analysis can be used to detect behavioral changes in elderly individuals [5], [6], or to identify errors in industrial assembly tasks [7]–[9].

In the offline setting, action recognition and action detection emerge as the primary tasks in analyzing trimmed and untrimmed videos, respectively. Action recognition involves categorizing videos into predefined classes [10], [11], whereas action detection extends this by identifying the temporal boundaries of each action within the video [12], [13]. While the former pursues a straightforward goal, the latter benefits from the sequential nature of actions to enrich the temporal context, thereby reinforcing the robustness of the employed model and solution.

A key aspect of both tasks is the granularity of the action categories, which can significantly affect the performance and applicability of the model. The definition of the different action categories is typically left to the discretion of the dataset authors, resulting in varying levels of abstraction. For example, the task of *make coffee* may be decomposed into several steps involving different objects: *open coffee maker*, *place filter*, etc. While the coarse granularity is sufficient in some cases, certain applications may require additional refinement to achieve specific goals. For example, robotics applications often require more detailed annotations, including per-joint instructions.

This work presents an action recognition architecture that exploits both the hierarchical structure and the sequential execution of actions. To this end, we adopt a transformer encoder built on the basis of state-of-the-art methods [14]–[16] that use this architecture to model temporal dependencies. By exploiting the self-attention mechanism inherent in transformer architectures, this model exceeds previous methods such as 3D CNNs [17]–[19] and RNNs [20]–[22], which often face challenges in capturing long-range temporal dependencies.

The Transformer architecture [23], originally designed for natural language processing, has undergone numerous improvements in recent years [24]–[26]. These improvements have enabled the models to handle temporal dependencies more effectively and to capture contextual information within textual data. We explore the benefits of these models to incor-

porate contextual data for action recognition in two different ways. First, by evaluating the effect of rephrasing to enrich textual descriptions of past actions along with camera location information which is achieved by leveraging instructional models such as GPT-3.5 [24] and Llama 3 [27]. Second, by encoding textual data into feature vectors using transformer text encoders [26], [28]. By fusing contextual information in the form of text embeddings with visual features prior to classification, we improve the overall representation of the ongoing action, enabling more accurate action recognition.

Our model is trained with the dual objective of both coarse-grained and fine-grained action classification. The rationale behind this approach is rooted in the idea that learning both coarse-grained and fine-grained actions together facilitates the recognition of both. Previous studies [29], [30] have explored action hierarchies under the premise that hyperbolic geometry naturally encodes hierarchical structures. Other works [31], [32] exploit the goal of the video, *i.e.* a coarse-grained action, to improve action anticipation performance. In our method, we propose a joint loss function to allow the model to better discriminate fine-grained actions.

For experimentation, we extend the existing Toyota Smarthome Untrimmed (TSU) dataset [33], incorporating action hierarchies into Activities of Daily Living (ADL). The resulting dataset, the Hierarchical TSU dataset, is, to the best of our knowledge, the first hierarchical dataset for ADL. Additionally, we evaluate the proposed method on the Assembly101 [8] and IkeaASM [34] action recognition benchmarks to provide further insights on the benefits of incorporating contextual information and action hierarchies.

Our implementation and the extended annotations for the Hierarchical TSU dataset are publicly available on Github<sup>1</sup>.

In summary, the contributions of this paper are the following:

- We present the Hierarchical TSU dataset, an extension of the original TSU dataset [33], that incorporates coarse-grained annotations and contextual information. Additionally, we compare various strategies for generating textual descriptions of contextual data by leveraging previous actions and camera location.
- We introduce a novel vision-language transformer architecture for action recognition that leverages hierarchical and contextual information, leading to more accurate action classification. Our approach outperforms state-of-the-art action recognition models in Assembly101 and IkeaASM benchmarks and serves as a strong baseline for the Hierarchical TSU dataset.
- We conduct extensive experiments to demonstrate the effectiveness of our approach. In addition to outperforming existing methods, we present detailed ablation studies that analyze the contributions of each component, as well as the impact of hierarchical and contextual information, including the role of large language models and the

influence of the number of past actions, and of location data.

The remainder of the paper is structured as follows. Section II summarizes the latest related work. In Section IV we describe in detail the proposed method. The experiments and results, including details on the Hierarchical TSU dataset, are reported in Section V, followed by the ablation study in Section VI. Finally, the main conclusions of this work are discussed in Section VII.

## II. RELATED WORK

We present an overview of pertinent literature concerning action recognition, focusing on the integration of language models and hierarchical structures of actions as tools to enhance action recognition performance.

### A. Action Recognition

Action recognition involves the classification of the action class performed within a video clip. Over time, various methodologies have been devised, with 2D CNN methods relying on single-frame human-object interaction being deemed the least effective due to their lack of temporal context [35]. Temporal modeling stands as a crucial aspect of action recognition. While recurrent neural networks and 3D CNN based methods held sway for several years [17]–[22], [36], the advent of video transformers [14]–[16] has significantly enhanced temporal modeling capabilities.

Two primary categories of architectures emerge. The first one comprises end-to-end models such as ViViT [37] which uses a pure transformer architecture for video classification inspired by the advances in the image domain. Embeddings are extracted as non-overlapping tubelets that span both the spatial and temporal dimensions. In TimeSformer [38], a convolution-free approach was presented with a detailed study on self-attention schemes. Results from this study suggest that divided attention for spatial and temporal features leads to the best performance. Video Swin [39] explores the inductive bias of locality in video transformers by adapting the Swin transformer designed for the image domain [40]. MViT [41] employs multiscale feature hierarchies with a pyramid of feature activations, allowing effective modeling of simple low-level, and complex high-level visual information. MViTv2 [42] enhances its predecessor with decomposed relative positional embeddings and residual pooling connections.

The second category comprises temporal modeling transformers that use pre-trained feature extractors from large datasets such as Kinetics-400 [17] and ImageNet [43]. OadTR [14] focus on temporal modeling using decoded RGB frames and frozen frame-level feature extractors. In addition, optical flow is computed on the RGB data to improve accuracy. Similarly, TIM [44] uses frozen visual and audio encoders for feature extraction. Features include a timestamp provided by a Time Interval MLP, so that the model can be queried about the events at a given interval in a specific modality. Other approaches incorporate the vision transformer, ViT [45], to fine-tune the feature extractor on the corresponding datasets [10],

<sup>1</sup><https://github.com/3dperceptionlab/HierarchicalActionRecognition>

[11], [46], yielding better results with a remarkable increase in terms of computing cost.

Feature extractors usually consist of 2D or 3D CNNs such as ResNet [47], InceptionV3 [48] or I3D [17]. On the contrary, MM-Vit [16] diverges by operating on multimodal features extracted from compressed videos, including I-frames, motion vectors and audio features. Similar strategies are observed in [49]–[51].

### B. Language Models for Action Recognition

The remarkable capabilities of large language models in temporal modeling and feature representation have been thoroughly investigated in recent years [24]–[26]. These capabilities have found application in various vision tasks, notably in image and video captioning. These approaches focus on generating textual descriptions of videos [52]. Recently, research has explored the use of language models to improve action recognition results. For example, ActionCLIP [10] uses a contrastive learning approach inspired by CLIP [53]. Instead of image captions, action classes are converted to prompts, which are then compared to the aggregated representation of a video. Spatial features from frames are extracted from a fine-tuned version of CLIP’s visual encoder, based on ViT [45]. Similarly, VideoCLIP [54] extends this learning paradigm to various video understanding tasks. Building on these advances, Text4Vis [11], [46] proposes to initialize a frozen classifier for action recognition using text embeddings derived from language models. Moreover, BIKE [55] introduces a novel framework that facilitates bi-directional cross-model knowledge transfer from vision to language models, with the aim of improving action recognition in videos.

Furthermore, the capabilities of language models in capturing temporal dependencies and contextual understanding have been exploited to model past actions as well [56]. VLMAH [57] presents a visual-linguistic approach to modeling action history that is particularly useful for instructional videos due to the sequential nature of the actions. Similarly, Furnari and Farinella [58] use “rolling-unrolling” LSTMs to succinctly summarize past actions. In contrast, AntGPT [32] exploits large language models for in-context learning [24] long-term action anticipation, *i.e.* by providing few ground-truth examples. Similarly, Zhang et al. [59] explore the benefits of incorporating object representations for this task. Encoded representations of cropped objects from RGB frames, along with bounding boxes and object labels encoded as text embeddings, are shown to improve the model’s performance.

### C. Action Hierarchies

Hierarchical structures have been explored in various ways for action understanding tasks, such as modeling features at multiple levels [13], [60]–[62] or leveraging annotations with varying granularity. In this work, we focus on the latter to investigate the potential of structured datasets for improving action understanding.

While current action recognition techniques have made significant progress, they often fall short in segmenting ac-

tions into distinct phases, which is required for many real-world applications. To address this gap, the authors of the FineGym dataset [63] introduced a sports video dataset with a three-level semantic hierarchy. Previous research [29], [30] has explored this dataset using the premise that hyperbolic geometry inherently encodes hierarchical structures. Using the Poincaré ball, these studies define a distance metric between predictions and observations, where points closer to the center of the ball represent abstract embeddings, while those near the edge denote specific ones. Essentially, edge proximity indicates higher model confidence.

Alternatively, Timeception [64] redefines the notion of activity, restricting it to “complex actions” characterized by: (1) composition - consisting of several simpler actions, (2) temporal order of these actions, and (3) extent - recognizing the variability in temporal length between actions. By introducing the Timeception layer, the architecture tolerates both long-range temporal dependencies and variations in the temporal extent.

The previously introduced AntGPT [32] also benefits from hierarchical information by incorporating goal information extracted from past actions using a large language model. A large language model is used to extract these goals in the form of text embeddings, which are then fused with visual observations to enhance long-term action anticipation. To generate hierarchical labels, AntGPT relies on twelve in-context examples, either manually curated or pseudo-labeled using large language models applied to video titles or descriptions. Similarly, in [31], authors exploit the goal concept to improve action anticipation in industrial scenarios by introducing a consistency loss to ensure alignment between coarse-grained and fine-grained predictions.

The industrial domain has particularly benefited from hierarchical annotations [8], [34], which may be explicitly provided or derived by defining coarse-grained related goals (e.g., assembling or disassembling a product). Other domains, such as autonomous driving, have also explored hierarchical annotations to capture the progression from high-level driving maneuvers to specific low-level actions [65].

Despite these advances, it is important to note the scarcity of annotated hierarchical data in the ADL domain, which prompts researchers in [29] to manually extend existing datasets for experimentation. Alternatively, synthetic data generators, such as Virtualhome [66], offer a hierarchical approach to generating video data, providing a valuable resource to address this limitation.

## III. HIERARCHICAL TSU DATASET

We introduce the Hierarchical TSU dataset, an extension of the Toyota Smarthome Untrimmed dataset [33], designed for the study of action hierarchies in activities of daily living. This dataset aims to incorporate and evaluate two complementary sources of information for action recognition: (1) contextual cues, such as prior actions, spatial location, and scene context, and (2) hierarchical organization of actions, reflecting the natural structure of human behavior.

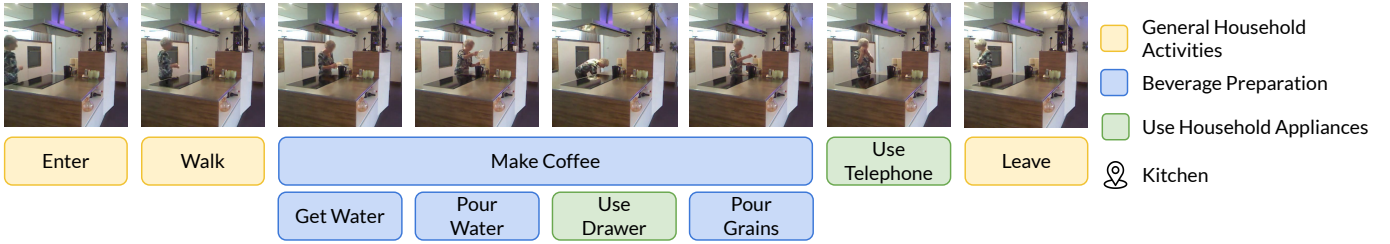


Fig. 1. **Hierarchical annotation example in the TSU dataset.** Video frames are annotated with fine-grained action labels, including composite activities (e.g., *Make coffee*). Each color corresponds to one of the coarse-grained action categories.

We adopt the TSU dataset as the foundation for our work due to several key advantages. Unlike other ADL datasets (e.g., Toyota Smarthome [67] or ETRI-Activity [68]), TSU provides temporally ordered annotations of actions, static camera viewpoints with known spatial locations, and a comprehensive taxonomy of fine-grained action labels. Specifically, it includes 51 distinct action classes recorded from 7 fixed cameras in various rooms of a house. The dataset features 536 untrimmed videos, each averaging 21 minutes in duration, and captures daily activities performed by 18 elderly individuals aged 60 to 80. This diversity in subject demographics and household settings makes TSU particularly well-suited for hierarchical and context-aware action recognition. In total, TSU contains over 64,000 annotated fine-grained action segments, which correspond to the trimmed action segments that compose the Hierarchical TSU dataset.

Among the 51 annotated actions are elementary activities such as *walk* and *get water*, as well as composite actions like *make coffee* and *cook*, which often encompass or temporally overlap with elementary actions. Although these composite and elementary actions exhibit clear hierarchical relationships, we preserve the original flat annotation structure of the TSU dataset to maintain consistency. Building upon this, we introduce an additional semantic layer by organizing the 51 action classes into a two-level hierarchy. Specifically, we manually assign each fine-grained action to one of seven coarse-grained categories, based on contextual semantics, location of execution, and visual similarity. The resulting high-level categories are: *beverage preparation*, *general household activities*, *cleaning*, *prepare breakfast*, *use household appliances*, *cook*, and *drink*. Table I summarizes the distribution of fine-grained actions within each coarse-grained category, as well as the number of annotated segments per class. While our work focuses on action recognition, we note that the introduced hierarchical annotations are also well-suited for action detection tasks within the TSU setup, as they enable richer temporal modeling and more structured predictions.

For contextual action recognition, we extract trimmed segments corresponding to individual fine-grained actions from the untrimmed videos. Because composite activities may span or overlap multiple fine-grained segments, the dataset includes overlapping annotations at both hierarchical levels, as illustrated in Figure 1. To enrich the temporal context, we additionally process preceding actions in the sequence,

TABLE I  
DISTRIBUTION OF FINE-GRAINED ACTIONS PER COARSE-GRAINED CATEGORY.

Coarse-Grained	# Fine-Grained	Samples	Avg. Dur. (s)
Beverage Preparation	11	2263	6.4
General Household Activities	14	40779	7.8
Cleaning	5	3457	10.1
Prepare breakfast	5	3787	7.83
Use Household Appliances	7	5645	13.33
Cook	5	6242	7.83
Drink	4	5241	2.87

encoding them as textual input. Finally, the known spatial configuration of the cameras, detailed in [33], is leveraged to associate each action with its location, thereby providing valuable spatial context for downstream models.

#### IV. METHODOLOGY

We present the proposed method for action recognition using hierarchical action structures and contextual information. Figure 2 illustrates an overview of the proposed architecture.

##### A. Video Encoder

We adopt a standard Transformer’s encoder to model temporal dependencies as in [14]. As noted earlier, the self-attention mechanism in transformer architectures has significantly outperformed previous methods based on 3D CNNs and RNNs, especially in the context of temporal modeling for videos. This mechanism allows for more effective capture of long-range dependencies and complex temporal relationships within video sequences.

Given a trimmed video  $V = \{f_t\}_{t=-T}^0$  associated with a coarse-grained action, and one or more fine-grained actions, the frames  $f_t$  are grouped into blocks of size  $B$ , resulting in  $(T + 1)/B$  chunks. For each block, we use a frozen feature extractor to obtain spatial features from RGB and optical flow frames, and employ separate video encoders with the same structure for each modality. We use the central frame of the block for RGB features, and the  $B$  frames sequence for optical flow features. These features are mapped into a  $D$  dimensional feature space, which we can formalize as  $F = \{\mathcal{O}_t\}_{t=-T}^0 \in \mathbb{R}^{(T+1) \times D}$ , where  $\mathcal{O}_t$  represents the output token of the transformer encoder at time  $t$ .

We extend the feature vector with an additional learnable class token with  $\mathcal{O}_{CLS} \in \mathbb{R}^D$ . This token is used to learn the

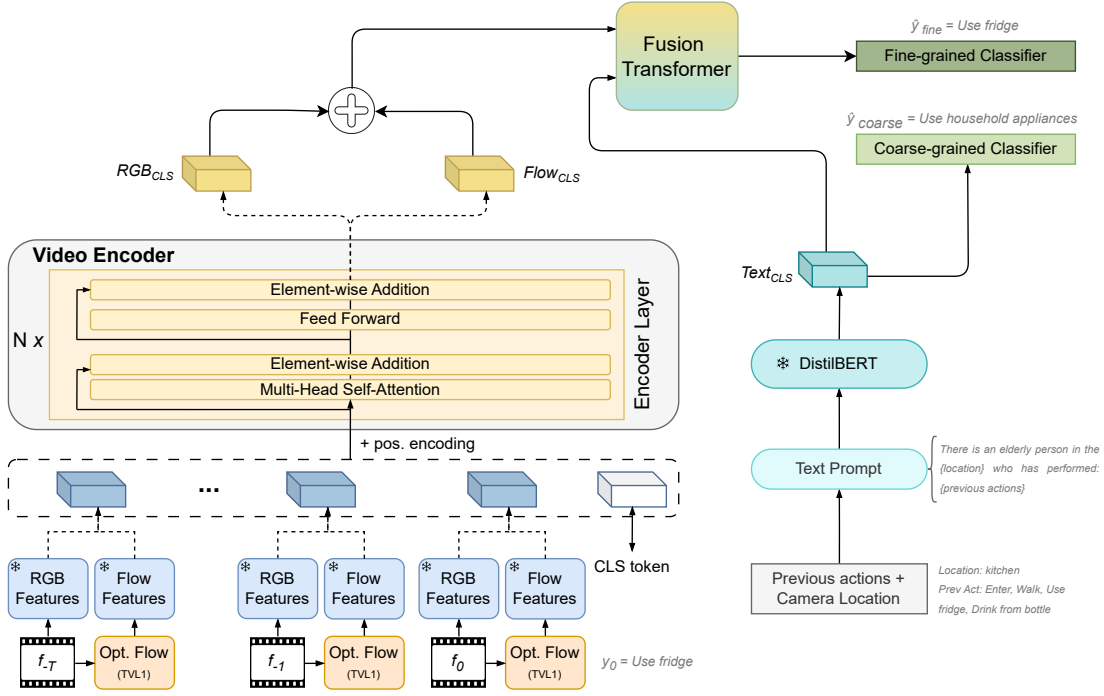


Fig. 2. **Overview of the proposed action recognition architecture.** From a video input, frozen feature extractors obtain spatial features from RGB frames and temporal motion features from optical flow. These features, along with a class token, are processed through individual video transformer encoders for each visual modality, capturing long-range temporal dependencies. Dashed lines indicate the use of either RGB or flow features and their respective embeddings, though only a single video encoder is depicted for simplicity. Additionally, DistilBERT extracts textual features that represent the current location, previous actions and dataset context. Coarse-grained actions are recognized based on contextual information, specifically utilizing the textual embeddings while the fine-grained classifier leverages the fused features from the fusion transformer.

aggregated representation of the entire input, and is combined with the feature sequence as  $\hat{F} = \text{Stack}(\{O_t\}_{t=-T}^0, O_{CLS}) \in \mathbb{R}^{(T+2) \times D}$ . Alternatively, the aggregated representation of the input can be obtained as the mean of the tokens in the input sequence as in [69].

Due to the lack of frame positional information in the encoder, we additionally embed positional encoding. Experiments comprise fixed sinusoidal inputs and trainable embeddings. We add positional encoding  $E_{pos} \in \mathbb{R}^{(T+2) \times D}$  as shown in Equation 1, *i.e.*, an element-wise addition to preserve positional information:

$$X_0 = \hat{F} + E_{pos}. \quad (1)$$

The fundamental element of the transformer model is the Multi-head Self-Attention (MSA) mechanism. In essence, self-attention enables each token to engage with others, enhancing its ability to gather valuable semantic insights. This process involves calculating dot products between queries and keys, followed by a softmax function to determine the importance assigned to each value. Formally,

$$X' = \text{Norm}(X_0), \quad (2)$$

$$\text{Attention}(Q_i, K_i, V_i) = \text{softmax}\left(\frac{Q_i K_i^T}{\sqrt{d_k}}\right) V_i, \quad (3)$$

$$H_i = \text{Attention}(Q_i, K_i, V_i), \quad (4)$$

where  $Q_i = X'W_i^q$ ,  $K_i = X'W_i^k$  and  $V_i = X'W_i^v$  are linear layers applied to the input sequence,  $W_i^q, W_i^k, W_i^v \in \mathbb{R}^{D \times \frac{D}{N_{head}}}$  with  $N_{head}$  represent the number of heads, and  $1/\sqrt{d_k}$  is a scaling factor that helps stabilizing the training and speed up convergence. Note that queries, keys and values are all vector representations. The outputs of each head are concatenated and fed into a linear layer as:

$$\hat{H} = \text{Stack}(H_1, H_2, \dots, H_{N_{head}})W_d \in \mathbb{R}^{(T+2) \times D}, \quad (5)$$

where  $W_d$  is a linear projection.

Finally, the output is fed into a two-layer feed-forward network (FFN) with GELU activation. Meanwhile, layer normalization and residual links are also applied. The video encoder formulas can then be summarized as follows:

$$\hat{H} = \text{MSA}(\text{Norm}(X_0)), \quad (6)$$

$$m'_1 = \hat{H} + X_0, \quad (7)$$

$$m_n = \text{FFN}(\text{Norm}(m'_{n-1})) + m'_{n-1}, \quad (8)$$

$$m'_n = \text{MSA}(\text{Norm}(m_{n-1})) + m_{n-1}, \quad (9)$$

where  $n \in N$  is the  $n$ -th encoder layer with a total of  $N$ ,  $m'$  denotes the output of the first element-wise addition in the encoder layer, and  $m_N \in \mathbb{R}^{(T+2) \times D}$  is the final feature representation of the last encoder layer. For the remaining of the paper, and for simplicity, we use  $m_{CLS} \in \mathbb{R}^D$  to denote the output representation of the class token from an encoder.

This notation is extended to  $m_{RGB}$  and  $m_{Flow}$  to refer to the same token of the respective modality.

### B. Contextualized Textual Information

Large language models have shown exceptional abilities in temporal modeling and context understanding. To leverage these capabilities, we propose an approach that models past information to enrich the contextualization of ongoing actions, thereby improving action recognition performance. Specifically, given the location and  $N$  previous actions, we use a prompt (as illustrated in Figure 2) to provide contextual information, including dataset domain (e.g. an elderly person), environment (e.g. camera location) and prior events, thus modeling longer temporal dependencies. From the generated sentences, we extract feature vectors using DistilBERT [28], a distilled variant of BERT [26], which employs deep bidirectional transformer encoders for text comprehension. As for the video encoder, we utilize the class token to represent the entire input sequence, denoted as  $m_{Txt}$ .

In addition to DistilBERT, we compare its performance against BERT and explore the use of LLMs for rephrasing to enhance data variability and richness. Section VI presents results for different setups, including no rephrasing, and rephrasing using GPT-3.5 [24] and Llama 3 [27], as well as an analysis of the optimal number of past actions and the influence of location information on contextualization.

1) *Exploiting Hierarchical Information from Context*: Contextual information derived from past actions and location provides a general understanding of the ongoing action, effectively yielding a coarse-grained representation. Likewise, this coarse-grained action can serve as supplementary supervision, enhancing fine-grained action recognition performance. To leverage this relationship, we introduce a coarse-grained classifier, which, in conjunction with a joint loss function, improves the accuracy of fine-grained action recognition.

2) *Fusion of Visual and Textual Embeddings*: In addition to their capabilities in temporal aggregation, transformer architectures excel at fusing features from different modalities [70]. To leverage this advantage, we employ a transformer encoder to combine visual and textual embeddings. Specifically, we concatenate RGB and optical flow features, as this approach has shown improved performance compared to feeding them separately into the fusion transformer. The encoder layers are structured similarly to the video encoder, but without the class token or positional encoding. Formally,

$$m_{VIS} = m_{RGB} + m_{Flow}, \quad (10)$$

$$m_M = \text{FusionTransformer}(m_{VIS}, m_{Txt}), \quad (11)$$

where  $m_{VIS} \in \mathbb{R}^{2 \times D}$  represents the combined RGB and optical flow features which are then mapped to the embedding space of the fusion transformer, denoted as  $\hat{D}$ . The output  $m_M \in \mathbb{R}^{2 \times \hat{D}}$  results from the  $M$  layer of the fusion transformer. The final representation from the fusion transformer, obtained as the mean of the output tokens, is denoted as  $m_{Fus}$ .

### C. Training

The model is trained on a dual classification objective. First, a fine-grained classifier uses  $m_{Fus}$  as input. Second, a coarse-grained classifier leverages contextual information from  $m_{Txt}$ . The resulting logits from both classifiers are used for multi-class classification, given the existing overlaps between composite actions, as discussed in the next section.

The supervision of both fine-grained and coarse-grained actions is performed through a joint loss function, defined as:

$$\mathcal{L} = BCE(\sigma(z_{coarse}), y_{coarse}) + BCE(\sigma(z_{fine}), y_{fine}), \quad (12)$$

where  $z$  and  $y$  represent predicted logits and ground truth labels, respectively. The function BCE denotes the binary cross-entropy loss, and  $\sigma$  is the sigmoid activation function applied to the logits. Using this combined formulation ensures numerical stability by applying the sigmoid and binary cross-entropy operations together, rather than separately.

## V. EXPERIMENTS

This section presents the experimental setup and results to demonstrate the effectiveness of the proposed method compared to the equivalent visual-only approach, and state-of-the-art methods across different datasets.

### A. Experimental Setup

**Evaluation:** We evaluate the results of our experiments on top- $k$  accuracy following previous work on action recognition [8], [10], [11], [34], [67]. Top- $k$  accuracy measures how often the correct action label appears among the top- $k$  labels predicted by the model. We use the cross-subject evaluation introduced in the TSU dataset [33], which uses 11 subjects for training and the remaining 7 for testing. Unless specified otherwise, in all tables, the best performance is highlighted in bold, and the best performance within each subgroup, if applicable, is underlined.

**Implementation details:** After exhaustive ablation experiments to determine the best configuration, we adopt ViT-H [45] with a patch size of 14 as RGB feature extractor and Inception v3 [48] from the two-stream network TSN [71] for optical flow features. TLV1 algorithm is used to compute optical flow frames. To extract embedding vectors from textual data we use DistilBERT [28].

The video encoder is composed of 4 attention layers with a single attention head, and an embedding size of 2048. The input vector is supplemented with learned position encoding and a CLS token. The resulting RGB and optical flow video embeddings are concatenated, and this visual representation is fused with text embeddings using the fusion transformer composed of 2 encoder layers, with 2 attention heads per layer and an embedding size of 768. The best performance is obtained using 32 blocks as input, which corresponds to 6.4 seconds of video. The prompt for contextual information contains 5 past actions along with location data.

**Training details:** The proposed method is implemented using PyTorch, and all experiments are conducted on Nvidia RTX

4090 GPUs. We employ AdamW optimizer with a weight decay of 0.1 and a base learning rate of  $5 \times 10^{-5}$ . Models are trained for 100 epochs with a batch size of 32, employing an early stopping mechanism with a patience of 20 epochs. We use gradient clipping to avoid exploding gradients and warm up the learning rate for 5 epochs. We set the block size to 5, which implies a downsampling rate of 5 on the 25 fps videos from the TSU dataset.

### B. Results

To determine the best combination of visual input with contextual data that provides the best top- $k$  accuracy, Table II presents the results for the best settings obtained after extensive ablation experiments (see Section VI).

For each experiment, we evaluate using both a fine-grained-only training objective (-), and a dual training objective with the proposed joint loss ( $\checkmark$ ). The results lead to the conclusion that the proposed method outperforms the standard approach relying only on visual inputs. Moreover, for every input combination it is observed that predicting both fine- and coarse-grained actions results in better performance. Note that the observed decrease in top-5 accuracy in some cases is primarily due to the model’s high confidence in the top classes.

**Impact of optical flow on video analytics:** Optical flow is considered an auxiliary modality that complements RGB data, providing a notable performance boost of 1.97% when used in combination with RGB, and even outperforming in the uni-modal approach (1.26%). However, its effectiveness diminishes when combined with contextual information and underperforms compared to the corresponding RGB-based method. When all three modalities (RGB, optical flow, and contextual information) are combined, optical flow contributes only a marginal improvement of 0.15%.

**On the effect of the joint loss function:** Using a joint loss function to predict both fine-grained and coarse-grained actions during training enhances performance across all input modalities. This approach yields up to a 1.37% improvement when fusing RGB and text embeddings. Notably, the top- $k$  performance of the coarse-grained classifier correlates with improvements in fine-grained action recognition.

**On the effect of exploiting contextual data:** Contextual data, which includes information about previous actions and location in text format, is dependent on visual observations from past frames. As a result, it is always combined with visual modalities and not used independently. Our results demonstrate that incorporating contextual data significantly enhances performance, yielding a 17.12% improvement compared to the RGB-only fine-grained approach, and outperforming all other fusion combinations.

To further validate the efficacy of the proposed method, we evaluate the best-performing model using contextual data extracted from its own predictions instead of ground truth annotations. Table III presents the top- $k$  accuracy for both fine- and coarse-grained actions. The results demonstrate the robustness of the method, even when relying on inference

TABLE II  
COMPARISON OF RESULTS: INPUT MODALITIES AND JOINT LOSS ON THE BEST SETTINGS.

Modalities	Joint Loss	Fine-Grained		Coarse-Grained	
		Top-1	Top-5	Top-1	Top-5
RGB	-	37.83	72.69	-	-
	$\checkmark$	<b>38.27</b>	73.55	75.62	99.41
Flow	-	39.09	72.69	-	-
	$\checkmark$	<b>39.39</b>	69.95	75.18	99.07
RGB + Flow	-	39.90	72.66	-	-
	$\checkmark$	<b>40.24</b>	74.21	75.44	99.37
RGB + Text	-	53.43	84.03	-	-
	$\checkmark$	<b>54.80</b>	84.37	<b>75.77</b>	99.37
Flow + Text	-	50.83	79.44	-	-
	$\checkmark$	<b>50.91</b>	81.07	75.29	99.56
RGB + Flow + Text	-	53.98	84.36	-	-
	$\checkmark$	<b>54.95</b>	84.11	73.77	99.15

TABLE III  
ACTION RECOGNITION PERFORMANCE WHEN CONTEXTUAL DATA ARE OBTAINED FROM PREDICTIONS.

Modalities	Fine Grained		Coarse Grained	
	Top-1	Top-5	Top-1	Top-5
RGB + Text	40.35	71.92	70.88	98.04
Flow + Text	41.42	70.99	70.43	97.85
RGB + Flow + Text	<b>43.16</b>	71.21	66.54	97.81

results. Compared to the previous joint loss results without contextual data, our method achieves a 2.08% improvement with RGB data, a 2.03% improvement with optical flow data, and a 2.92% improvement with the combined RGB and optical flow approach.

### C. Comparison with State-of-the-art Methods

To evaluate the reliability and robustness of our approach, we compare our method with existing state-of-the-art architectures for action recognition. Given that this work introduces the Hierarchical TSU dataset, the results serve as a baseline to evaluate where our method stands relative to existing approaches. To this end, we train state-of-the-art methods for action recognition initialized with pre-trained Kinetics 400 [17] weights for 100 epochs, matching the training duration of our proposed method. 3D CNN models, including VideoResNet [72], SlowFast [36], and X3D [73], are trained using the Adam optimizer with a learning rate of  $10^{-4}$ , as this configuration showed improved performance for these architectures. Transformer-based models, consisting of Video Swin [39], MViT [41], [42], TimeSformer [38] and ViVit [37], are trained using the same hyperparameters as our method for consistency. To provide a fair comparison across architectures, we evaluate performance using input sizes that match those required by the respective state-of-the-art models.

Table IV summarizes the findings, demonstrating that our model outperforms both 3D CNN and transformer-based architectures on the Hierarchical TSU dataset when trained under identical input size and hyperparameter settings. The best performance, achieved using ground truth contextual data, is highlighted in bold, while the second-best results, derived from

TABLE IV  
COMPARISON TO STATE-OF-THE-ART METHODS TRAINED ON THE  
HIERARCHICAL TSU DATASET.

Model	# Input Blocks	Top-1	Top-5
X3D [73]		30.22	67.05
MViT (Base) [41]		33.01	70.28
MViTv2 (Small) [42]	16	32.47	70.80
TimeSformer [38]		30.87	66.53
<u>Ours</u> (Predictions)		<u>37.98</u>	67.55
<b>Ours</b> (Ground Truth)		<b>51.14</b>	81.02
VideoResNet [72]		36.72	75.70
SlowFast [36]		36.53	68.77
Video Swin (Base) [39]		36.42	74.18
Video Swin (Small) [39]		37.05	74.32
Video Swin (Tiny) [39]	32	36.75	70.32
TimeSformer [38]		37.31	70.32
ViVit [37]		37.76	69.62
<u>Ours</u> (Predictions)		<u>43.16</u>	71.21
<b>Ours</b> (Ground Truth)		<b>54.95</b>	84.11

inference contextual data, are underlined for each number of input blocks.

#### D. Evaluation across Datasets

We further evaluate the proposed method on two additional action recognition benchmarks, IkeaASM and Assembly101. These industrial-like datasets are chosen for their inclusion of key elements relevant to our approach: untrimmed videos that support contextual modeling of prior actions, and hierarchical action structures.

**IkeaASM** [34]: This dataset focuses on furniture assembly tasks in different settings comprising 33 atomic (fine-grained) actions under 4 high-level (coarse-grained) categories, each consisting of a different furniture type. Unlike the Hierarchical TSU, a single fine-grained class is assigned to multiple coarse-grained classes. We follow the default train/test data split using the *top* camera view to ensure comparability with prior work. The model architecture and feature extractors match the best settings on the Hierarchical TSU. Given the absence of known locations, we exclude location information from the prompt, and adapt the domain information to “*a person building furniture*”. Results are presented in Table V, following [34] we report Top-1/3 accuracy.

**Assembly101** [8]: This large-scale dataset captures the procedural assembly and disassembly of toy vehicles. It includes 1380 fine-grained and 199 coarse-grained action classes. Similar to IkeaASM, the dataset allows a fine-grained action to be associated with multiple coarse-grained categories, as fine- and coarse-grained recognition tasks are treated independently. To establish fine-to-coarse relationships in this dataset, we matched corresponding temporal segments.

We use the default train/test split and employ the provided DINOv2 [74] RGB features from the v4 camera for comparison, which yields the best performance in the third-person view. Because the features are pre-extracted, optical flow is not used, otherwise, the model setup remains the same. As with IkeaASM, prompts omit location information, and the domain context is described as “*a person assembling a toy.*” The results are reported in Table VI.

TABLE V  
ABLATION AND COMPARISON TO STATE-OF-THE-ART METHODS ON  
IKEAASM DATASET. SOTA EXTRACTED FROM [34]. VISUAL: RGB +  
FLOW. CONTEXTUAL: RGB + FLOW + TEXT.

Model	Hier?	Top-1	Top-3
Ours (Visual)	-	<u>75.77</u>	83.68
	✓	<u>75.43</u>	<u>84.54</u>
Ours (Contextual)	-	<u>76.98</u>	<u>88.49</u>
	✓	<u>79.04</u>	76.98
C3D [75]	-	45.73	69.56
P3D [76]	-	60.40	81.07
I3D [17]	-	57.58	76.72
Multimodal (RGB, Pose, Depth) [34]	-	64.02	81.45
Ours (Contextual from predictions)	✓	<b>65.29</b>	81.96

TABLE VI  
ABLATION AND COMPARISON TO STATE-OF-THE-ART METHODS ON  
ASSEMBLY101 DATASET. SOTA EXTRACTED FROM [8]. VISUAL: RGB.  
CONTEXTUAL: RGB + TEXT.

Model	Hier?	Top-1	Top-5
Ours (Visual)	-	72.98	84.25
	✓	<u>73.06</u>	<u>83.96</u>
Ours (Contextual)	-	<u>81.44</u>	89.80
	✓	<u>81.89</u>	<u>89.41</u>
TSM [77]	-	38.3	-
TempAgg [78]	-	40.5	-
Ours (Contextual from predictions)	✓	<b>43.47</b>	69.48

Results on both benchmarks demonstrate the effectiveness of the proposed method over prior work (see the second half of Table V and Table VI). On IkeaASM, our method using contextual information from predictions achieves an improvement of nearly 5% in Top-1 accuracy over the previous state-of-the-art RGB-based method, and over 1% compared to a multimodal approach that combines RGB, depth and 3D pose data. On Assembly101, it yields almost a 3% gain in Top-1 accuracy compared to TempAgg [78]. The ablation studies in the first half of the same tables further highlight the impact of contextual modeling, showcasing the benefits of leveraging longer temporal cues and introducing domain-specific textual information.

In contrast, incorporating hierarchical structures results in only marginal improvement on Assembly101 and even a slight decrease in performance on IkeaASM. We attribute this drop to label ambiguity. In IkeaASM, fine-grained actions are commonly assigned to multiple, or even all, coarse-grained categories, making the hierarchy noisy and less informative. As previously discussed, the hierarchical structure in IkeaASM was not designed explicitly for hierarchical action recognition but rather to organize the data by furniture type. Similarly, in Assembly101, hierarchical labels are treated as a separate task rather than an intrinsic semantic structure. Consequently, instead of guiding the model, these hierarchies can introduce noise and hinder fine-grained recognition. This effect is more pronounced in IkeaASM and only mildly beneficial in Assembly101, where over 50% of coarse-grained classes share at least one fine-grained action, and only 25% of fine-grained actions are uniquely assigned. These results underscore the

TABLE VII

COMPUTATIONAL REQUIREMENTS OF STATE-OF-THE-ART METHODS (*S*: Small, *B*: Base).

Method	# Frames	Trainable Params (M)	Total Params (M)	GFlops (Inference)
X3D		3.08	3.08	10.04
MViT (B)	16	36.34	36.34	141.8
MViTv2 (S)		34.27	34.27	128.64
VideoResNet		33.19	33.19	25.44
SlowFast		34.6	34.6	1970
VideoSwin (S)	32	49.55	49.55	244.66
TimeSformer		121.4	121.4	1519.3
ViVit		88.69	88.69	906.52
Ours		143.06	306.11	610.4

importance of a well-structured and semantically meaningful label hierarchy in action understanding datasets, as unclear or overlapping hierarchies can negatively impact performance.

### E. Computational Analysis

We conduct a comparative analysis of the computational characteristics with respect to the previously introduced baseline methods in Table VII. Compared to prior works, our model shows a larger learning capacity, reflected in a higher number of trainable parameters, while maintaining a lower inference cost. Methods based on CNN architectures have lighter computational requirements, but they generally underperform compared to transformer-based approaches. In contrast, our method achieves substantially better accuracy than other transformer-based models while requiring less computations during inference. Specifically, our model comprises 143.06 million trainable parameters, augmented by an additional 86.39 million parameters from RGB feature extraction, 10.3 million from optical flow feature extraction and 66.36 million from the transformer textual encoder. These parameters were obtained using the feature extractors that performed best.

In terms of inference complexity, our approach requires 13.78 GFLOPs for the multimodal fusion and classification. The visual feature extraction cost is calculated as  $(33.74 + 2.85) \times 32$  GFLOPs, accounting for both the RGB and optical flow pathways across 32 frames. Additionally, the textual encoding incurs a cost of 11.18 GFLOPs. Overall, this leads to a substantially lower computational cost compared to transformer-based methods like TimeSformer and ViVit, or CNN-based approaches such as SlowFast, which process a larger number of frames or use additional frames to capture richer temporal cues despite similar input window sizes.

## VI. ABLATION EXPERIMENTS

We present an ablation study to assess the contributions of the individual components within our proposed method. In addition to identifying the optimal RGB feature extractor and determining the best configuration values for the transformers used in the architecture, we compare various approaches for incorporating hierarchical information. We also analyze the influence of the number of past actions and the inclusion of location data within the contextual information. Furthermore, we

TABLE VIII

EFFECT OF REPHRASING AND COMPARISON OF TEXT FEATURE EXTRACTORS.

Feature Extractor	Rephrasing	Top-1	Top-5
BERT	GPT 3.5	39.46	73.14
	Llama 3	40.79	75.18
DistilBERT	-	40.53	75.36
	GPT 3.5	48.50	80.47
DistilBERT	Llama 3	49.20	79.84
	-	<b>54.95</b>	84.11

TABLE IX

STUDY ON THE NUMBER OF PAST ACTIONS AND EFFECT OF LOCATION ON CONTEXTUAL DATA.

# Past Actions	Location	Top-1	Top-5
1	-	49.17	82.33
	✓	<u>50.87</u>	84.25
3	-	<u>52.58</u>	84.29
	✓	51.80	84.70
5	-	53.46	84.18
	✓	<b>54.95</b>	84.11
7	-	<u>52.46</u>	82.33
	✓	50.95	80.81

investigate the impact of rephrasing with GPT-3.5 and Llama 3 on enriching contextual data, as well as the effect of different text encoders. Unless specified otherwise, all experiments in this section are conducted using the best configuration settings, which result in a 54.95% top-1 accuracy, and we report the outcomes on fine-grained action recognition.

### A. Contextual Data Analysis

The best performing model considers the last 5 actions and the location provided by fixed cameras as contextual data. Text embeddings are obtained using DistilBERT [28] for feature extraction and the *prompt* used to generate the descriptions is a fixed template. Table VIII compares the use of DistilBERT and BERT as feature extractors as well as the use of rephrasing to enhance textual descriptions exploiting two well known large language models: GPT3.5 and Llama 3.

Results indicate that DistilBERT outperforms its predecessor for feature extraction. Additionally, a notable improvement is observed when using DistilBERT with a fixed template, as opposed to rephrasing for enhancing textual descriptions.

Based on the optimal configuration, we conducted a study to determine the best number of past actions and assess the impact of location on contextual descriptions. The results, presented in Table IX, suggest that using five past actions yields the best performance on the Hierarchical TSU dataset. Regarding location information, we observe that it provides improvements only when using 1 or 5 past actions, with variability in other cases.

### B. Strategies for Hierarchical Action Recognition

As discussed in Section IV, fine-grained action recognition is performed using fused embeddings that combine both visual and contextual information. In addition, we compare different strategies for integrating fine-grained and coarse-grained

TABLE X

COMPARISON OF STRATEGIES FOR HIERARCHICAL ACTION RECOGNITION.

Method	Fine-Grained		Coarse-Grained	
	Top-1	Top-5	Top-1	Top-5
(1) Contextual Data	<b>54.95</b>	84.11	73.77	99.15
(2) Separate Fusion	51.83	82.14	73.10	99.19
(3) Separate Classifier	51.24	81.88	74.21	99.11
(4) Shared Classifier	48.17	78.55	73.18	99.44

TABLE XI

COMPARISON OF FUSION STRATEGIES.

Method	Top-1	Top-5
(1) Separate Modalities	49.94	80.03
(2) Visual Concat	<b>54.95</b>	84.11
(3) Concat	40.53	74.25

action recognition into a joint learning framework. Table X presents the results of four mechanisms, each depending on the features used to disambiguate fine- and coarse-grained information. Specifically, the strategies are: (1) using only contextual information for coarse-grained action recognition; (2) using two separate fusion transformers, employing the same visual and contextual features as the fine-grained classifier; (3) using two separate classifiers from the same fused embeddings for fine- and coarse-grained classification; and (4) sharing part of the classifier layers, while separating only the final classification layers.

The results indicate that the differentiation between fine-grained and coarse-grained features plays a significant role in performance. Specifically, using only contextual information for coarse-grained action recognition (1) achieves the best performance, with a top-1 accuracy of 54.95% for fine-grained actions and competitive results for coarse-grained actions. This suggests that contextual data is particularly effective for coarse-grained recognition and also helps to improve fine-grained action accuracy.

Although the use of contextual data improves coarse-grained recognition, it does not achieve the highest top-1 accuracy. However, it remains competitive compared to other approaches. We attribute this to the role of coarse-grained actions as an auxiliary modality that primarily enhances fine-grained performance, rather than being the main focus of the model. The highest top-1 accuracy for coarse-grained actions is achieved when incorporating visual information, as seen in the separate classifier strategy (3), which yields the best performance for coarse-grained recognition.

Furthermore, strategies (2)-(4), which involve increasing the number of shared layers between fine-grained and coarse-grained actions, lead to a reduction in fine-grained accuracy. We argue that this occurs because fine-grained actions rely on more detailed, discriminative visual features, while coarse-grained actions benefit from broader, higher-level visual cues.

### C. Data Fusion

Effective fusion of data modalities is crucial for achieving strong model performance. To this end, we evaluate three

TABLE XII

ABLATION STUDY ON THE NUMBER OF ENCODER LAYERS ON THE FUSION TRANSFORMER.

# Enc. Layers	Top-1	Top-5
1	54.80	84.81
2	<b>54.95</b>	84.11
3	51.32	81.96
4	50.46	82.07

TABLE XIII

ABLATION STUDY ON THE NUMBER OF ATTENTION HEADS ON THE FUSION TRANSFORMER.

# Att. Heads	Top-1	Top-5
1	53.21	83.70
2	<b>54.95</b>	84.11
4	52.02	83.22
6	51.32	82.81
8	53.61	83.70

different fusion strategies and conduct an ablation study on the most effective one: the fusion transformer. RGB and optical flow features are obtained separately, based on the finding that late fusion is the best strategy for the video encoder, as discussed in the next section. We assess the impact of three approaches: (1) concatenating all three modalities (RGB, optical flow, and text), (2) concatenating the visual modalities (RGB and optical flow) prior to the fusion transformer, and (3) inputting the three modalities separately. Table XI contains the results, with visual concatenation prior to the fusion transformer performing best on top-1 accuracy.

Since the fusion transformer outperforms the concatenation approach, we conduct an ablation study on the number of attention heads and encoder layers, while keeping the embedding size fixed at 768, which corresponds to the text modality. Table XII presents the results for different numbers of encoder layers, with two layers yielding the best performance. Similarly, Table XIII shows the results for varying numbers of attention heads, with two heads being the optimal configuration for our method.

### D. Video Transformer

We determine the optimal configuration for the video encoder by evaluating several factors: input length, RGB feature extractor, number of layers and attention heads, fusion strategy, embedding size, and the use of positional encoding and CLS tokens.

**Input Length:** In theory, longer input sequences should improve action recognition accuracy, provided there is no data loss due to excessively long sequences. Table XIV shows the results of our experiments with different sequence lengths. Our findings indicate that an input length of 6.4 seconds (32 input blocks) yields the best performance. Longer sequences tend to miss specific actions within the dataset, while shorter sequences lack the temporal context needed for accurate recognition.

**RGB Feature Extractor:** Since transformer models for fea-

TABLE XIV  
ABLATION STUDY ON THE NUMBER OF INPUT BLOCKS.

# Input Blocks	Video duration (sec)	Top-1	Top-5
8	1.8	49.45	80.56
16	3.2	51.14	81.02
32	6.4	<b>54.95</b>	84.11
64	12.8	50.70	84.50

TABLE XV  
ABLATION STUDY ON RGB FEATURES EXTRACTORS.

Feature Extractor	Top-1	Top-5
Inception v3 [48]	47.57	77.81
BN-Inception [79]	48.54	79.33
ViT-H/14 [45]	<b>54.95</b>	84.11

ture extraction are typically trained on static images rather than videos, they may encounter challenges such as motion blur caused by moving objects or people. To address this, we experiment with ViT-H/14 [45] as well as RGB feature extractors from the two-stream network TSN [71], both using pre-trained weights from the Kinetics dataset [17]. Specifically, we evaluate Inception v3 [48] and BN-Inception [79]. As shown in Table XV, despite being trained on static images, the transformer-based method achieves the best accuracy.

**Positional Information:** As pointed out in Section IV, extracted frame features lack order information. Table XVI contains an ablation study on using fixed and learnable position encodings against not using them. Results show that positional encoding to preserve the order of the frames is necessary, and that learned positional encoding performs best.

**Number of Encoder Layers and Heads:** Finding a balance between the number of encoding layers and attention heads plays a critical role in the performance of transformer models. In Table XVII results show that 4 encoding layers is the best value for this task. Similarly, Table XVIII shows that the model accuracy improves when using a single attention head.

**Embedding Size and Visual Fusion Strategy:** We experiment with three different embedding dimensions on two visual fusion strategies: early and late. Early fusion involves concatenating feature vectors before the input to the transformer encoder. In contrast, a late fusion strategy requires two video encoders, one for RGB features and one for optical flow features. The results are shown in Table XIX, with late fusion and an embedding size of 2048 providing the best top-1 accuracy.

**Encoder Representations:** The output of the transformer encoder provides a representation for each input token. To avoid biasing the model towards a particular video block, we experiment with two different representations as explained in Section IV. As shown in Table XX, using a class token improves the encoder’s representation, resulting in a more robust model compared to the mean of each of the encoder’s output tokens.

TABLE XVI  
ABLATION STUDY ON POSITION ENCODING

Positional Encoding	Top-1	Top-5
-	44.31	76.33
Fixed	52.21	82.96
Learnable	<b>54.95</b>	84.11

TABLE XVII  
ABLATION STUDY ON THE NUMBER OF ENCODER LAYERS.

# Enc. Layers	Top-1	Top-5
2	52.76	82.07
4	<b>54.95</b>	84.11
6	54.50	84.18
8	54.76	83.03

TABLE XVIII  
ABLATION STUDY ON THE NUMBER OF ATTENTION HEADS.

# Att. Heads	Top-1	Top-5
1	<b>54.95</b>	84.11
2	52.02	81.92
4	44.98	76.58
8	42.91	74.84
16	42.65	75.84

TABLE XIX  
ABLATION STUDY ON THE EMBEDDING DIMENSION AND VISUAL FUSION STRATEGIES.

Fusion Type	Embedding Size	Top-1	Top-5
Early	768	43.98	73.18
	1024	44.35	75.81
	2048	<u>53.72</u>	83.96
Late	768	45.35	77.36
	1024	45.94	76.47
	2048	<b>54.95</b>	84.11

TABLE XX  
ABLATION STUDY ON THE ENCODER REPRESENTATION.

Encoder Representation	Top-1	Top-5
CLS token	<b>54.95</b>	84.11
Mean	45.72	78.21

## VII. CONCLUSION

In this work, we proposed a method that effectively leverages both contextual information from past actions, location and domain information, and the hierarchical structure of actions, to improve action recognition accuracy.

To fully leverage these contextual and structural cues, we propose the Hierarchical TSU dataset, an extension of the original TSU with a two-level annotation hierarchy and enriched contextual labels. This dataset supports a more comprehensive evaluation of hierarchical and context-aware action recognition methods.

Through extensive experimentation on the proposed Hierarchical TSU dataset, as well as two additional benchmarks, IkeaASM and Assembly101, we demonstrate that long-term contextual information can be successfully aggregated using language models. In addition, when available, contextual cues such as environment and current location, if available, further contribute to improving action recognition performance.

Hierarchical structures also lead to improvements, although their impact is generally smaller compared to contextual information. Our results highlight the importance of adequately structuring action annotations to fully exploit hierarchical relationships.

## ACKNOWLEDGMENT

This work has been funded by the Valencian regional government CIAICO/2022/132 Consolidated group project AI4Health, and by the Spanish State Research Agency (AEI) and ERDF/EU under grant: GEMELIA PID2024-161711OB-I00. This work is also a part of the ENIA Chair of Artificial Intelligence from the University of Alicante (TSI100927-2023-6) funded by the Recovery, Transformation and Resilience Plan from the European Union Next Generation through the Ministry for Digital Transformation and the Civil Service. This work has also been supported by a Spanish national and two regional grants for PhD studies, FPU21/00414, CIACIF/2021/430 and CIACIF/2022/175.

## REFERENCES

- [1] P. Ni, S. Lv, X. Zhu, Q. Cao, and W. Zhang, "A light-weight online action detection with hand trajectories for industrial surveillance," *Digital Communications and Networks*, vol. 7, no. 1, pp. 157–166, 2021.
- [2] J. Kim, T. Misu, Y.-T. Chen, A. Tawari, and J. Canny, "Grounding human-to-vehicle advice for self-driving vehicles," in *CVPR*, June 2019.
- [3] V. Ramanishka, Y.-T. Chen, T. Misu, and K. Saenko, "Toward driving scene understanding: A dataset for learning driver behavior and causal reasoning," in *CVPR*, 2018.
- [4] L. Tong, H. Ma, Q. Lin, J. He, and L. Peng, "A novel deep learning bi-gru-i model for real-time human activity recognition using inertial sensors," *IEEE Sensors Journal*, vol. 22, no. 6, pp. 6164–6174, 2022.
- [5] E. Talavera, C. Wuerich, N. Petkov, and P. Radeva, "Topic modelling for routine discovery from egocentric photo-streams," *Pattern Recognition*, vol. 104, p. 107330, 2020.
- [6] M. Menchón, E. Talavera, J. Massa, and P. Radeva, "Behavioural patterns discovery for lifestyle analysis from egocentric photo-streams," *Pervasive and Mobile Computing*, vol. 95, p. 101846, 2023.
- [7] A. Flaborea, G. M. D. di Melendugno, L. Plini, L. Scofano, E. De Matteis, A. Furnari, G. M. Farinella, and F. Galasso, "Prego: Online mistake detection in procedural egocentric videos," in *Proceedings of the IEEE/CVF Conference on Computer Vision and Pattern Recognition (CVPR)*, June 2024, pp. 18 483–18 492.

- [8] F. Sener, D. Chatterjee, D. Shelepov, K. He, D. Singhanian, R. Wang, and A. Yao, "Assembly101: A large-scale multi-view video dataset for understanding procedural activities," in *Proceedings of the IEEE/CVF Conference on Computer Vision and Pattern Recognition (CVPR)*, June 2022, pp. 21 096–21 106.
- [9] T. J. Schoonbeek, T. Houben, H. Onvlee, P. H. de With, and F. van der Sommen, "Industreal: A dataset for procedure step recognition handling execution errors in egocentric videos in an industrial-like setting," in *Proceedings of the IEEE/CVF Winter Conference on Applications of Computer Vision (WACV)*, January 2024, pp. 4365–4374.
- [10] M. Wang, J. Xing, and Y. Liu, "Actionclip: A new paradigm for video action recognition," 2021.
- [11] W. Wu, Z. Sun, and W. Ouyang, "Revisiting classifier: Transferring vision-language models for video recognition," in *Proceedings of the AAAI Conference on Artificial Intelligence*, vol. 37, 2023, pp. 2847–2855.
- [12] R. Dai, S. Das, K. Kahatapitiya, M. S. Ryoo, and F. Brémond, "Ms-tct: Multi-scale temporal convtransformer for action detection," in *Proceedings of the IEEE/CVF Conference on Computer Vision and Pattern Recognition*, 2022, pp. 20 041–20 051.
- [13] R. Dai, S. Das, L. Minciullo, L. Garattoni, G. Francesca, and F. Brémond, "Pdan: Pyramid dilated attention network for action detection," in *Proceedings of the IEEE/CVF Winter Conference on Applications of Computer Vision*, 2021, pp. 2970–2979.
- [14] X. Wang, S. Zhang, Z. Qing, Y. Shao, Z. Zuo, C. Gao, and N. Sang, "Oadtr: Online action detection with transformers," in *ICCV*, October 2021, pp. 7565–7575.
- [15] A. Ulhaq, N. Akhtar, G. Pogrebna, and A. Mian, "Vision transformers for action recognition: A survey," *arXiv:2209.05700*, 2022.
- [16] J. Chen and C. M. Ho, "Mm-vit: Multi-modal video transformer for compressed video action recognition," in *Proceedings of the IEEE/CVF Winter Conference on Applications of Computer Vision (WACV)*, January 2022, pp. 1910–1921.
- [17] J. Carreira and A. Zisserman, "Quo vadis, action recognition? a new model and the kinetics dataset," in *2017 IEEE Conference on Computer Vision and Pattern Recognition (CVPR)*, 2017, pp. 4724–4733.
- [18] M. Fayyaz, E. Bahrami, A. Diba, M. Noroozi, E. Adeli, L. V. Gool, and J. Gall, "3d cnns with adaptive temporal feature resolutions," in *CVPR*, 2021.
- [19] M. E. Kalfaoglu, S. Kalkan, and A. A. Alatan, "Late temporal modeling in 3d cnn architectures with bert for action recognition," in *Computer Vision – ECCV 2020 Workshops*, 2020, pp. 731–747.
- [20] Z. Li, K. Gavriilyuk, E. Gavves, M. Jain, and C. G. Snoek, "VideoLstm convolves, attends and flows for action recognition," *Computer Vision and Image Understanding*, vol. 166, pp. 41–50, 2018.
- [21] J.-Y. He, X. Wu, Z.-Q. Cheng, Z. Yuan, and Y.-G. Jiang, "Db-lstm: Densely-connected bi-directional lstm for human action recognition," *Neurocomputing*, vol. 444, pp. 319–331, 2021.
- [22] J. An, H. Kang, S. H. Han, M.-H. Yang, and S. J. Kim, "Miniroad: Minimal rnn framework for online action detection," in *ICCV*, October 2023, pp. 10 341–10 350.
- [23] A. Vaswani, N. Shazeer, N. Parmar, J. Uszkoreit, L. Jones, A. N. Gomez, E. Kaiser, and I. Polosukhin, "Attention is all you need," *Advances in neural information processing systems*, vol. 30, 2017.
- [24] T. B. Brown, B. Mann, N. Ryder *et al.*, "Language models are few-shot learners," 2020.
- [25] H. Touvron, L. Martin, K. Stone *et al.*, "Llama 2: Open foundation and fine-tuned chat models," 2023.
- [26] J. Devlin, M.-W. Chang, K. Lee, and K. Toutanova, "Bert: Pre-training of deep bidirectional transformers for language understanding," *arXiv:1810.04805*, 2018.
- [27] A. Dubey, A. Jauhri, A. Pandey, A. Kadian *et al.*, "The llama 3 herd of models," 2024. [Online]. Available: <https://arxiv.org/abs/2407.21783>
- [28] V. Sanh, "Distilbert, a distilled version of bert: Smaller, faster, cheaper and lighter," *arXiv preprint arXiv:1910.01108*, 2019.
- [29] D. Suris, R. Liu, and C. Vondrick, "Learning the predictability of the future," *arXiv:2101.01600*, 2021.
- [30] J.-A. Castro-Vargas, A. Garcia-Garcia, P. Martinez-Gonzalez, S. Oprea, and J. Garcia-Rodriguez, "Unsupervised hyperbolic action recognition," in *ROBOT2022*, 2023, pp. 479–488.
- [31] O. Zatsarynna and J. Gall, "Action anticipation with goal consistency," in *2023 IEEE International Conference on Image Processing (ICIP)*, 2023, pp. 1630–1634.

- [32] Q. Zhao, S. Wang, C. Zhang, C. Fu, M. Q. Do, N. Agarwal, K. Lee, and C. Sun, "Antgpt: Can large language models help long-term action anticipation from videos?" *ICLR*, 2024.
- [33] R. Dai, S. Das, S. Sharma, L. Minciullo, L. Garattoni, F. Bremond, and G. Francesca, "Toyota smarthome untrimmed: Real-world untrimmed videos for activity detection," *TPAMI*, pp. 1–1, 2022.
- [34] Y. Ben-Shabat, X. Yu, F. Saleh, D. Campbell, C. Rodriguez-Opazo, H. Li, and S. Gould, "The ikea asm dataset: Understanding people assembling furniture through actions, objects and pose," in *Proceedings of the IEEE/CVF Winter Conference on Applications of Computer Vision (WACV)*, January 2021, pp. 847–859.
- [35] M. Benavent-Lledo, S. Oprea, J. A. Castro-Vargas, D. Mulero-Perez, and J. Garcia-Rodriguez, "Predicting human-object interactions in egocentric videos," in *2022 International Joint Conference on Neural Networks (IJCNN)*, 2022, pp. 1–7.
- [36] C. Feichtenhofer, H. Fan, J. Malik, and K. He, "Slowfast networks for video recognition," in *Proceedings of the IEEE/CVF International Conference on Computer Vision (ICCV)*, October 2019.
- [37] A. Arnab, M. Deghani, G. Heigold, C. Sun, M. Lučić, and C. Schmid, "Vivit: A video vision transformer," in *Proceedings of the IEEE/CVF international conference on computer vision*, 2021, pp. 6836–6846.
- [38] G. Bertasius, H. Wang, and L. Torresani, "Is space-time attention all you need for video understanding?" in *Proceedings of the International Conference on Machine Learning (ICML)*, July 2021.
- [39] Z. Liu, J. Ning, Y. Cao, Y. Wei, Z. Zhang, S. Lin, and H. Hu, "Video swin transformer," in *Proceedings of the IEEE/CVF conference on computer vision and pattern recognition*, 2022, pp. 3202–3211.
- [40] Z. Liu, Y. Lin, Y. Cao, H. Hu, Y. Wei, Z. Zhang, S. Lin, and B. Guo, "Swin transformer: Hierarchical vision transformer using shifted windows," in *Proceedings of the IEEE/CVF International Conference on Computer Vision (ICCV)*, October 2021, pp. 10012–10022.
- [41] H. Fan, B. Xiong, K. Mangalam, Y. Li, Z. Yan, J. Malik, and C. Feichtenhofer, "Multiscale vision transformers," in *ICCV*, 2021.
- [42] Y. Li, C.-Y. Wu, H. Fan, K. Mangalam, B. Xiong, J. Malik, and C. Feichtenhofer, "Mvitv2: Improved multiscale vision transformers for classification and detection," in *CVPR*, 2022.
- [43] J. Deng, W. Dong, R. Socher, L.-J. Li, K. Li, and L. Fei-Fei, "Imagenet: A large-scale hierarchical image database," in *2009 IEEE Conference on Computer Vision and Pattern Recognition*, 2009, pp. 248–255.
- [44] J. Chalk, J. Huh, E. Kazakos, A. Zisserman, and D. Damen, "Tim: A time interval machine for audio-visual action recognition," *arXiv:2404.05559*, 2024.
- [45] A. Dosovitskiy, L. Beyer, A. Kolesnikov, D. Weissenborn, X. Zhai, T. Unterthiner, M. Deghani, M. Minderer, G. Heigold, S. Gelly *et al.*, "An image is worth 16x16 words: Transformers for image recognition at scale," *arXiv:2010.11929*, 2020.
- [46] W. Wu, Z. Sun, Y. Song, J. Wang, and W. Ouyang, "Transferring vision-language models for visual recognition: A classifier perspective," *International Journal of Computer Vision*, pp. 1–18, 2023.
- [47] K. He, X. Zhang, S. Ren, and J. Sun, "Deep residual learning for image recognition," in *Proceedings of the IEEE conference on computer vision and pattern recognition*, 2016, pp. 770–778.
- [48] C. Szegedy, V. Vanhoucke, S. Ioffe, J. Shlens, and Z. Wojna, "Rethinking the inception architecture for computer vision," in *Proceedings of the IEEE conference on computer vision and pattern recognition*, 2016, pp. 2818–2826.
- [49] Y. Ming, L. Xiong, X. Jia, Q. Zheng, and J. Zhou, "Fsconformer: A frequency-spatial-domain cnn-transformer two-stream network for compressed video action recognition," in *2023 IEEE Smart World Congress (SWC)*. IEEE, 2023, pp. 838–843.
- [50] J. Wang and L. Torresani, "Deformable video transformer," in *CVPR*, 2022, pp. 14053–14062.
- [51] Y. Ming, J. Zhou, N. Hu, F. Feng, P. Zhao, B. Lyu, and H. Yu, "Action recognition in compressed domains: A survey," *Neurocomputing*, vol. 577, p. 127389, 2024.
- [52] S. Li, Z. Tao, K. Li, and Y. Fu, "Visual to text: Survey of image and video captioning," *IEEE Transactions on Emerging Topics in Computational Intelligence*, vol. 3, no. 4, pp. 297–312, 2019.
- [53] A. Radford, J. W. Kim, C. Hallacy, A. Ramesh, G. Goh, S. Agarwal, G. Sastry, A. Askell, P. Mishkin, J. Clark, G. Krueger, and I. Sutskever, "Learning transferable visual models from natural language supervision," 2021.
- [54] H. Xu, G. Ghosh, P.-Y. Huang, D. Okhonko, A. Aghajanyan, F. Metze, L. Zettlemoyer, and C. Feichtenhofer, "Videoclip: Contrastive pre-training for zero-shot video-text understanding," *arXiv:2109.14084*, 2021.
- [55] W. Wu, X. Wang, H. Luo, J. Wang, Y. Yang, and W. Ouyang, "Bidirectional cross-modal knowledge exploration for video recognition with pre-trained vision-language models," in *Proceedings of the IEEE/CVF Conference on Computer Vision and Pattern Recognition*, 2023.
- [56] A. Caesar, O. Özdemir, C. Weber, and S. Wermter, "Enabling action crossmodality for a pretrained large language model," *Natural Language Processing Journal*, p. 100072, 2024.
- [57] V. Manousaki, K. Bacharidis, K. Papoutsakis, and A. Argyros, "Vlmah: Visual-linguistic modeling of action history for effective action anticipation," in *Proceedings of the IEEE/CVF International Conference on Computer Vision*, 2023, pp. 1917–1927.
- [58] A. Furnari and G. M. Farinella, "Rolling-unrolling lstms for action anticipation from first-person video," *IEEE transactions on pattern analysis and machine intelligence*, vol. 43, no. 11, pp. 4021–4036, 2020.
- [59] C. Zhang, C. Fu, S. Wang, N. Agarwal, K. Lee, C. Choi, and C. Sun, "Object-centric video representation for long-term action anticipation," in *2024 IEEE/CVF Winter Conference on Applications of Computer Vision (WACV)*, 2024, pp. 6737–6747.
- [60] M. M. Islam and T. Iqbal, "Hamlet: A hierarchical multimodal attention-based human activity recognition algorithm," in *2020 IEEE/RSJ International Conference on Intelligent Robots and Systems (IROS)*, 2020, pp. 10 285–10 292.
- [61] A. Richard, H. Kuehne, and J. Gall, "Weakly supervised action learning with rnn based fine-to-coarse modeling," in *Proceedings of the IEEE Conference on Computer Vision and Pattern Recognition (CVPR)*, July 2017.
- [62] S. Cao, Z. Zhang, J. Jiao, J. Qiao, G. Song, and R. Shen, "Mcaf: Efficient agent-based video understanding framework through multimodal coarse-to-fine attention focusing," *arXiv preprint arXiv:2504.17213*, 2025.
- [63] D. Shao, Y. Zhao, B. Dai, and D. Lin, "Finegym: A hierarchical video dataset for fine-grained action understanding," in *IEEE Conference on Computer Vision and Pattern Recognition (CVPR)*, 2020.
- [64] N. Hussein, E. Gavves, and A. W. Smeulders, "Timeception for complex action recognition," in *Proceedings of the IEEE/CVF Conference on Computer Vision and Pattern Recognition (CVPR)*, June 2019.
- [65] M. Martin, A. Roitberg, M. Haurilet, M. Horne, S. Reiss, M. Voit, and R. Stiefelwagen, "Drive&act: A multi-modal dataset for fine-grained driver behavior recognition in autonomous vehicles," in *Proceedings of the IEEE/CVF International Conference on Computer Vision (ICCV)*, October 2019.
- [66] X. Puig, K. Ra, M. Boben, J. Li, T. Wang, S. Fidler, and A. Torralba, "Virtualhome: Simulating household activities via programs," in *Proceedings of the IEEE Conference on Computer Vision and Pattern Recognition*, 2018, pp. 8494–8502.
- [67] S. Das, R. Dai, M. Koperski, L. Minciullo, L. Garattoni, F. Bremond, and G. Francesca, "Toyota smarthome: Real-world activities of daily living," in *2019 IEEE/CVF International Conference on Computer Vision (ICCV)*, 2019, pp. 833–842.
- [68] J. Jang, D. Kim, C. Park, M. Jang, J. Lee, and J. Kim, "Etri-activity3d: A large-scale rgb-d dataset for robots to recognize daily activities of the elderly," in *2020 IEEE/RSJ International Conference on Intelligent Robots and Systems (IROS)*. IEEE, 2020, pp. 10 990–10 997.
- [69] L. Beyer, X. Zhai, and A. Kolesnikov, "Better plain vit baselines for imagenet-1k," 2022.
- [70] P. Xu, X. Zhu, and D. A. Clifton, "Multimodal learning with transformers: A survey," *IEEE Transactions on Pattern Analysis and Machine Intelligence*, vol. 45, no. 10, pp. 12 113–12 132, 2023.
- [71] L. Wang, Y. Xiong, Z. Wang, Y. Qiao, D. Lin, X. Tang, and L. Val Gool, "Temporal segment networks: Towards good practices for deep action recognition," in *ECCV*, 2016.
- [72] D. Tran, H. Wang, L. Torresani, J. Ray, Y. LeCun, and M. Paluri, "A closer look at spatiotemporal convolutions for action recognition," in *Proceedings of the IEEE Conference on Computer Vision and Pattern Recognition (CVPR)*, June 2018.
- [73] C. Feichtenhofer, "X3d: Expanding architectures for efficient video recognition," in *Proceedings of the IEEE/CVF Conference on Computer Vision and Pattern Recognition (CVPR)*, June 2020.
- [74] M. Oquab, T. Darcet, T. Moutakanni, H. Vo, M. Szafraniec, V. Khalidov, P. Fernandez, D. Haziza, F. Massa, A. El-Nouby *et al.*, "Dinov2: Learning robust visual features without supervision," *arXiv preprint arXiv:2304.07193*, 2023.

- [75] D. Tran, L. Bourdev, R. Fergus, L. Torresani, and M. Paluri, "Learning spatiotemporal features with 3d convolutional networks," in *Proceedings of the IEEE international conference on computer vision*, 2015, pp. 4489–4497.
- [76] Z. Qiu, T. Yao, and T. Mei, "Learning spatio-temporal representation with pseudo-3d residual networks," in *proceedings of the IEEE International Conference on Computer Vision*, 2017, pp. 5533–5541.
- [77] J. Lin, C. Gan, and S. Han, "Tsm: Temporal shift module for efficient video understanding," in *Proceedings of the IEEE/CVF international conference on computer vision*, 2019, pp. 7083–7093.
- [78] F. Sener, D. Singhania, and A. Yao, "Temporal aggregate representations for long-range video understanding," in *Computer Vision–ECCV 2020: 16th European Conference, Glasgow, UK, August 23–28, 2020, Proceedings, Part XVI 16*. Springer, 2020, pp. 154–171.
- [79] S. Ioffe and C. Szegedy, "Batch normalization: Accelerating deep network training by reducing internal covariate shift," in *International conference on machine learning*. pmlr, 2015, pp. 448–456.